DATE: 2018/05/29
VERSION: 5

Title: Pan-cancer machine learning predictors of tissue of origin and molecular subtype

Authors

Author	Symbol
William F. Flynn	1¶
Sandeep Namburi	1¶
Carolyn A. Paisie	1
Honey V. Reddi	1,2
Sheng Li	1,2*
R. Krishna Murthy Karuturi	1,2*
Joshy George	1,2*

Affiliations

1. The Jackson Laboratory for Genomic Medicine, 10 Discovery Drive, Farmington, Connecticut, USA

2. The Jackson Laboratory Cancer Center, Bar Harbor, Maine, USA

¶ These authors contributed equally to this work.

* Corresponding Authors: sheng.li@jax.org, krishna.karuturi@jax.org, joshy.george@jax.org

ABSTRACT

Background: It is estimated by the American Cancer Society that approximately 5% of all metastatic tumors have no defined primary tissue of origin and are classified as *cancers of unknown primary origin* (CUPs). The current standard of care for CUP patients depends on immunohistochemistry (IHC) based approaches to identify the primary site. The addition of post-mortem evaluation to IHC based tests helps to reveal the identity of the primary site for only 25% of the CUPs, emphasizing the acute need for better methods of determination of the site of origin. CUP patients are therefore given generic chemotherapeutic agents resulting in poor prognosis. When the tissue of origin is known, patients can be given site specific therapy with significant improvement in clinical outcome. Similarly, identifying the primary origin of metastatic cancer is of great importance for designing treatment.

Identification of the primary site of origin is an import first step but may not be sufficient information for optimal treatment of the patient. Recent studies, primarily from The Cancer Genome Atlas (TCGA) project, and others, have revealed molecular subtypes in several cancer types with distinct clinical outcome. The molecular subtype captures the fundamental mechanisms driving the cancer and provides information that is essential for the optimal treatment of a cancer. Thus, along with primary site of origin, molecular subtype of a tumor is emerging as a criterion for personalized medicine and patient entry into clinical trials.

However, there is no comprehensive toolset available for precise identification of tissue of origin or molecular subtype for precision medicine and translational research.

Methods and Findings: We posited that metastatic tumors will harbor the gene expression profiles of the primary tissue of origin of the cancer. Therefore, we decided to learn the characteristics of the primary tumors using the large number of cancer genome profiles

available from the TCGA project. Our predictors were trained for 33 cancer types and for the 11 cancers where there are established molecular subtypes. We estimated the accuracy of several machine learning models using cross-validation methods and external validation sets. The extensive testing using independent test sets revealed that the predictors had a median sensitivity and specificity of 97.2% and 99.9% respectively without losing classification of any tumor. Subtype classifiers achieved median sensitivity of 87.7% and specificity of 94.5% via cross validation and presented median sensitivity of 79.6% and specificity of 94.6% in two external datasets of 1,999 total samples. Importantly, these external data shows that our classifiers can robustly predict the cancer primary origin from microarray data, metastatic cancer, and patient-derived xenograft (PDX) mouse models.

Conclusion: We have demonstrated the utility of gene expression profiles to solve the important clinical challenge of identifying the primary site of origin and the molecular subtype of cancers based on machine learning algorithms. We show, for the first time to our knowledge, that our pan-cancer classifiers can predict multiple cancers' primary tissue of origin from metastatic samples. The predictors will be made available as open source software, freely available for academic non-commercial use.

KEYWORDS

Cancer, TCGA, RNA-seq, Classification, Subtypes, Transcriptome, Machine learning, Cell-of-origin, Cancer-of-unknown-primary

1. INTRODUCTION

Precision cancer therapy requires the knowledge of tissue of origin and accurate subtyping of the cancer to identify an appropriate therapeutic regimen. However, according to the American Cancer Society, an estimated 2 to 5 percent of all cancer patients have metastatic tumors for which routine testing cannot locate the primary site and is therefore classified as a cancer of unknown primary (CUP). CUP patients have very poor prognosis, primarily because the course of treatment is generic and not tailored for a specific tumor type [1, 2]. In addition, lack of knowledge of the cause of the disease puts CUP patients under severe psychological distress that may lead to clinically significant depressive symptoms [3].

In a study of CUP patients that were predicted to have primary tumors originating in the colon, the median survival of patients increased in those that received site-specific chemotherapy as compared to those who received empirically-determined treatments [4, 5]. Furthermore, multiple studies have supported the use of molecular profiling to diagnose CUP and to determine specific treatment based upon the predicted tissue of origin leading to an improvement in overall survival [6-9]. Therefore, it is important to develop systematic methods to identify the primary site of origin of the disease.

Currently, immunohistochemistry (IHC) utilizing antibodies targeted to certain tumor-specific antigens is the main method for primary tumor identification in patients with CUP [2, 10]. However, there is not a single, specific marker that can be used to conclusively diagnose the primary tumor, leading to the use of multiple different IHC markers, and generating the possibility that different clinicians will arrive at different diagnoses of the primary tumor type [2, 11-14]. Recent advances in genomics has led to the development of potential new means for diagnosing these tumors; multiple studies have utilized gene expression profiles and other molecular markers to diagnose CUP [2]. One such method involved comparisons of gene

90 expression profiles between CUPs and a set of primary and metastatic tumors with known
91 origins to predict the tissue of origin for the CUP [2, 6, 15-20]. None of these tools were able to
92 identify the tissue of origin with high sensitivity and specificity for all the CUP samples. For
93 example, the EPICUP tool, which had the best performance to date provides high accuracy for
94 only 87% of the CUP samples.
95
96 Several studies, including the Cancer Genome Atlas (TCGA) and International Cancer Genome
97 Consortium (ICGC) studies, have shown that the cancers from the primary tissue can be
98 classified into molecular subtypes with distinct clinical outcome and therapeutic options [21-28].
99 The molecular subtype information can also have predictive power. For example, Bevacizumab,
100 a monoclonal antibody that block angiogenesis, is shown to benefit patients of mesenchymal
101 and proliferative subtypes in ovarian cancer and therefore may be used as a criterion for the
102 entry into a clinical trial [29]. In addition, molecular subtype information can guide the selection
103 of targeted therapies and to suggest new treatment strategies (e.g. the potential use of JAK2
104 inhibitors and PD-L1/2 antagonists for the treatment of EBV-positive gastric cancer) [27].
105 However, identification of molecular subtypes is clinically challenging and thus clinicians are
106 unable to utilize molecular subtype information to inform treatment decisions [30, 31] due to a
107 lack of tools and assays for pan-cancer subtyping despite the availability of genomic
108 technologies for clinical diagnostics.
109
110 To fill this important gap in the clinical and translational research setting, using expression data
111 available from the TCGA project, we developed Machine Learning based predictors that enable
112 accurate identification of tissue of origin and subtype of cancer (Figure 1). Our predictors were
113 trained for 33 cancer types and for the 11 cancers where there are established molecular
114 subtypes. The extensive testing using independent test sets revealed that the predictors had a
115 median sensitivity and specificity of 97.2% and 99.9% respectively without losing classification

116 of any tumor using in total 1,959 samples. Subtype classifiers achieved median sensitivity of
117 79.6% and specificity of 94.6% using two external validation sets consisting of 1,999 breast and
118 ovarian cancer samples in total. Our gene expression-based pan-cancer classifier can, for the
119 first time to our knowledge, robustly predict multiple cancers' primary tissue of origin from
120 metastatic samples using an independent validation dataset (specificity: 99.3%, sensitivity:
121 82.1%). Compared to other pan-cancer classifiers based on somatic mutations, our classifier is
122 not limited to only cancer types with high mutation burden and has much greater potential for
123 clinical diagnosis and therapeutic design.
124

125 ## 2. METHODS

126 ### 2.1 Expression datasets

127 #### 2.1.1 Learning set: TCGA expression data

128 RSEM [32] normalized mRNA expression matrices were downloaded for each of the 33 unique
129 cancer cohorts (listed in Table 1) available from the Broad Institute GDAC Firehose (run
130 2016_01_28) [33]. Individual cohort expression matrices were converted to Biobase
131 ExpressionSet objects [34] for standardization and then combined as an ExpressionSet stored
132 in Apache Feather format (version 0.4.0) to allow downstream analysis in both R and Python
133 (https://github.com/wesm/feather). The raw expression matrix consisted 11,330 samples and
134 20,531 genes, which was reduced to 10,446 samples and 9,642 genes after filtering (detailed
135 below).
136
137 **Table 1. 33 GDAC Cancer Cohorts**

Cohort Abbr.	Cases	Disease Name
ACC	92	Adrenocortical carcinoma
BLCA	412	Bladder urothelial carcinoma
BRCA	1,098	Breast invasive carcinoma
CESC	307	Cervical and endocervical cancers
CHOL	51	Cholangiocarcinoma
COAD	460	Colon adenocarcinoma
DLBC	58	Lymphoid Neoplasm Diffuse Large B-cell Lymphoma

ESCA	185	Esophageal carcinoma
GBM	613	Glioblastoma multiforme
HNSC	528	Head and Neck squamous cell carcinoma
KICH	113	Kidney Chromophobe
KIRC	537	Kidney renal clear cell carcinoma
KIRP	323	Kidney renal papillary cell carcinoma
LAML	200	Acute Myeloid Leukemia
LGG	516	Brain Lower Grade Glioma
LIHC	377	Liver hepatocellular carcinoma
LUAD	585	Lung adenocarcinoma
LUSC	504	Lung squamous cell carcinoma
MESO	87	Mesothelioma
OV	602	Ovarian serous cystadenocarcinoma
PAAD	185	Pancreatic adenocarcinoma
PCPG	179	Pheochromocytoma and Paraganglioma
PRAD	499	Prostate adenocarcinoma
READ	171	Rectum adenocarcinoma
SARC	261	Sarcoma
SKCM	470	Skin Cutaneous Melanoma
STAD	443	Stomach adenocarcinoma
TGCT	150	Testicular Germ Cell Tumors
THCA	503	Thyroid carcinoma
THYM	124	Thymoma
UCEC	560	Uterine Corpus Endometrial Carcinoma
UCS	57	Uterine Carcinosarcoma
UVM	80	Uveal Melanoma

138

139 **2.1.2 External validation data**

140 External cancer gene expression datasets, i.e. those used exclusively for testing the
141 performance of models, were obtained from the publicly available Gene Expression Omnibus
142 (GEO) and the patient-derived xenograft (PDX) mouse models generated at the Jackson
143 Laboratory. These datasets were not introduced during model fitting (hence external validation)
144 and were generated using both RNA-seq and microarray technologies.

145

146 The first dataset used to test the model accuracy was the microarray gene expression profile of
147 2,158 cancer samples from the expression project for oncology (expO, GSE2109) [35]. Of the
148 2,158 samples, we were able to identify relevant primary tumor types for 1,558 samples and
149 excluded LGG/GBM from classification due to too few samples, resulting in classification of
150 1,552 samples. The second dataset, GSE18549, contained expression profiles of 96 tumors

151 from their metastatic sites [36]. We used 88 of these tumors whose primary sites could be
152 identified and those with more than 1 sample per primary site. The third dataset used contains
153 the expression profile of 338 PDX RNA-seq samples generated at the Jackson Laboratory and
154 available through the Mouse Tumor Biology (MTB) gene expression portal
155 (http://tumor.informatics.jax.org) [37]. Of these 338 samples, 325 samples could be mapped to
156 one of the 33 TCGA primary cancer types and the 7 OV samples were excluded as they
157 originate from the same two patients. The distribution of the primary types in the external
158 datasets used for validation are shown in Table 2.
159
160 **Table 2. Distribution of samples in the three external datasets used to validate the**
161 **primary classification model**

	External dataset		
Primary site	GSE2109	GSE18549	PDX
BLCA	32	0	29
BRCA	354	14	41
COAD	312	35	68
DLBC	0	0	4
KIRC/KIRP/KIRH	281	6	8
LAML	0	0	13
LGG/GBM	6	0	5
LIHC	46	0	0
LUAD/LUSC	133	10	88
OV	279	14	7
PAAD	0	0	12
PRAD	83	9	0
READ	0	1	0
SARC	0	0	32
SKCM	0	0	18
THCA	32	0	0
N/A	600	7	13
Used	1,552	88	318
Total	2,158	96	338

162

163 For external validation of our subtype classifiers, we acquired two additional microarray
164 datasets. The first, accession number GSE9899, contains 215 ovarian cancer samples [15] and
165 the second, EGA study EGAS00000000083 (https://www.ebi.ac.uk/ega), contains 1,784 breast
166 cancer samples [38]. Both datasets comprise 4 molecular subtypes each: mesenchymal,
167 immunoreactive, differentiated, and proliferative for the ovarian set; and basal-like, HER2-
168 enriched, luminal A, and luminal B for the breast set.
169
170 **2.1.3 Normalization, filtering, and preprocessing**
171 All expression data was log2-transformed, and only genes with (a) maximum log2 expression
172 greater than 8 and (b) variance in log2 expression greater than 1 were retained. After filtering,
173 the genes in each dataset was scaled to zero mean expression and unit variance. This scaling
174 allows expression to be measured in terms of standard deviations and affords platform-
175 independent use of subsequently trained models.
176
177 **2.1.4 Molecular subtype label curation**
178 Molecular subtype information was downloaded from cBioPortal [39, 40] for 3,367 samples from
179 the following primary cancers: glioblastoma multiforme (GBM), stomach adenocarcinoma
180 (STAD), breast (BRCA), ovarian (OV), prostate (PRAD), and lung squamous cell cancers
181 (LUSC). Further annotations were curated from the following supplemental data files: lower
182 grade glioma (LGG) [41], head and neck squamous cell carcinoma (HNSC) [22], uterine corpus
183 endometrial carcinoma (UCEC) [42], cutaneous melanoma (SKCM) [43], papillary (KIRP) [44]
184 and clear cell (KIRC) [45] renal cancers, and lung adenocarcinoma (LUAD) [27]. R (version 3+)
185 scripts were written to extract relevant information (e.g. sample id, specific subtype) from
186 downloaded data and supplemental files. These scripts are available in the public project
187 GitHub repository as described under Code availability.

188

189 **2.1.5 Pan-organ group labels**

190 A recently published study performed integrated clustering on the multiomic data from the
191 roughly 10,000 The Cancer Genome Atlas (TCGA) samples of 33 types of cancer. The authors
192 identified multi-cancer groups, which tend to span whole organs or related organ groups [46].
193 We use these pan-organ groups assignments to present our classification results in a whole- or
194 multi-organ context and for logical grouping of primary cancer types in figures. These
195 classifications are reproduced here: central nervous system (GBM LGG), core gastrointestinal
196 (ESCA, STAD, COAD, READ), developmental gastrointestinal (LIHC, PAAD, CHOL), endocrine
197 (THCA and ACC), gynecologic (OV, UCEC CESC BRCA), head and neck (HNSC), hematologic
198 and lymphatic malignancies (LAML, DLBC, THYM), melanocytic (SKCM and UVM), neural-
199 crest-derived tissues (PCPG), soft tissue (SARC and UCS), thoracic (LUAD, LUSC, MESO),
200 urologic (BLCA, PRAD, TGCT, KIRC, KICH, KIRP).

201

202 **2.2 Machine Learning Algorithms for Cancer Classification**

203 We evaluated several popular machine learning algorithms to develop CUP classification and
204 subtype identification: DLDA, KNN, SVM and Random Forest. We used R-packages
205 *sparsediscrim* (version 0.2.4)*, base::knn, e1071* (version 1.6-8)*,* and *randomForest* (version 4.6-
206 14), respectively for the training, testing; and *caret* (version 6.0-79) for tool development.
207 Unless otherwise specified, default parameters were chosen for model construction.

208

209 **2.2.1 Diagonal Linear Discriminant Analysis (DLDA)**

210 The DLDA classifier belongs to the family of Naive Bayes classifiers, where the distribution of
211 each class is assumed to be a multivariate normal and to share a common covariance matrix.
212 The DLDA classifier is a modification to LDA, where the off-diagonal elements of the pooled

213 sample covariance matrix are set to zero [47]. DLDA was used as classifier in several genomic
214 based cancer classification tasks [48, 49].
215
216 **2.2.2 k-Nearest Neighbor (KNN) classifier**
217 A KNN classifier offers the simplest classifier training strategy, also referred to as 'lazy
218 classifier', and has been successfully applied in the classification of cancer and non-cancer
219 related classification tasks [50-52]. A KNN classifier uses the training set as reference vectors
220 and, for every sample in the test set, the k nearest (in Euclidean distance) training set vectors
221 are found. The classification is decided by majority vote of the k-nearest neighbors' class. Note
222 that, if multiple neighbor vectors are found with identical distances, all such neighbor vectors are
223 included in the voting pool, which can lead to k being exceeded in these cases [53].
224
225 **2.2.3 Support Vector Machine (SVM)**
226 The SVM algorithm builds a predictive model by constructing a representation of the training
227 samples as points in higher dimensional space and builds a linear model (separating linear
228 boundary) in that space such that the mapped samples of the different categories are separated
229 by a gap that is as wide as possible. New examples are then mapped into that same space and
230 predicted to belong to a category based on which side of the separating boundary they fall. For
231 multiclass classification among N classes, N*(N-1)/2 binary SVM classifiers are constructed and
232 trained in a one-versus-one manner; ultimate class predictions come from voting amongst the
233 ensemble of binary classifiers. The implementation used for our classifiers employed a
234 Gaussian kernel. SVMs were successfully used for classification of samples in variety of studies
235 [54-56].
236
237 **2.2.4 Random Forest**

238 The random forest algorithm employs a collection of decision trees constructed from
239 bootstrapped input data and classification is done by majority voting among the ensemble of
240 trees [57]. Single decision trees are prone to overfitting; multiple trees constructed from
241 randomly sampled copies of the input data allows the consensus classification to be robust and
242 extensible to new samples. Each of our random forest models constructed 1000 trees, each
243 tree constructed from randomly sampled input with replacement, and each decision tree node
244 uses 31 randomly selected features to partition the tree.
245
246 **2.3 Model training and external validation**
247 The schema for classifier design for tumor type classification and subtype classification are
248 depicted in Figure 1.
249
250 **2.3.1 Design of Tumor type classifier**
251 All models were trained using the same feature selection and cross-validation schedule. Each
252 model was then trained using a 3-fold cross validation procedure as follows. The expression set
253 is partitioned into 3 random subsamples and for each partition: (1) the selected partition is used
254 as the testing set and the remaining 9 are combined into a training set; (2) the 100 most
255 differentially expressed genes in each class (cancer type) are selected, measured by log-fold-
256 change of differential expression between in-class and out-of-class samples ($p < 0.001$); (3) the
257 model is trained using the selected features; (4) predictions for the selected partition is
258 recorded. The cross-validation procedure yields an estimate of the model performance with the
259 selected parameters. The final model is then constructed using the entire set of samples and
260 1,971 unique genes selected via the procedure in (2) above.
261
262 **2.3.2 Molecular subtype classification**

263 For each of the 11 primary cancer types with established molecular subtypes, a model is
264 constructed as described above using the scaled, log2-transformed expression of the sample
265 corresponding to the selected primary type as input. For each cancer type, similar to cancer
266 type classification, features are selected by computing the differential expression ($p<0.001$) in
267 each subtype in comparison with the other subtypes of the same cancer type.
268

269 **2.3.3 Comparison metrics**

270 Each classification algorithm was compared using per class and overall positive predictive
271 value, sensitivity, and specificity. Additional metrics such as per-class balance accuracy, and
272 F1 score are included in the supplementary tables. Per class metrics are computed using a
273 one-versus-all scheme.
274

275 **2.4 Visualization**

276 An interactive web application was constructed using the Python Dash framework (version
277 0.21.0). The application shows the TCGA data embedded in three dimensions using UMAP
278 (umap-learn, version 0.2.1, [58]) and t-SNE (MulticoreTSNE, version 0.1, [59, 60]). Data points
279 are color coded by tumor type (with cancer and match normal samples), cancer type, and
280 molecular subtype, which can be controlled interactively through the interface.
281

282 The web application and the associated code are freely available for non-commercial, academic
283 use at https://pccportal.jax.org (pan-cancer classification portal) and the source code is
284 available as described in the Code availability subsection.
285

286 **2.5 Code availability**

287 All code to download, process, train, and validate these data and models is

288 available in the following GitHub repository:

289 https://github.com/TheJacksonLaboratory/tcga_subtype_classification. All results and the

290 majority of figures can be easily reproduced by cloning and running make.

291

292 **3. RESULTS**

293 **3.1 Precise classification of primary cancer types across platforms**

294 The classification of the 33 primary cancer types from the TCGA cohort (9,642 samples) by

295 random forest is presented in Figure 2A. Classification yields a median sensitivity and

296 specificity of 97.2% and 99.9% (n=33), respectively (Figure 2C). The major misclassifications

297 are primarily within organ systems (Figure 2B). Indeed, when primary types are grouped by

298 pan-organ groups [46], the median sensitivity increases to 98.5% with a substantial

299 improvement in the minimum sensitivity to 86.0% (Figure 2B,D). It is important to note that

300 every sample was classified by our model; no samples were excluded from classification, either

301 by a sample quality metric or through lack of consensus during label assignment. The most

302 frequent misclassifications occur between nearby locations in the gastrointestinal tract; rectal

303 adenocarcinoma (READ) is completely misclassified as colon adenocarcinoma (COAD), and

304 esophageal carcinoma (ESCA) is often misclassified as stomach adenocarcinoma

305 (STAD). COAD and READ are so similar that they are typically considered as a single primary

306 type, colorectal carcinoma (CRC) [23]. Misclassification between ESCA and STAD is expected,

307 as a certain class of ESCAs (esophageal adenocarcinomas) present at the interface of the

308 esophagus and stomach [61]. Also of note is the misclassification of uterine carcinosarcoma

309 (UCS) as uterine corpus endometrial carcinoma (UCEC). Histologically, USC presents features

310 of both UCEC and sarcoma (SARC) [62].

311

312 To understand these misclassifications, the expression profiles of every training sample was

313 embedded into a two-dimensional latent space using UMAP (see Methods) and colored by

314 primary tumor type, shown in Figure 3. Several anatomical and histological structures readily
315 emerge from the embedding. Some cancers are observed to form disparate, well-separated
316 clusters by organ system, such as brain (GBM-LGG), liver and gallbladder (LIHC, CHOL), and
317 kidneys (KIRC, KIRP, KIRH), while other cancers are grouped by histological features, such as
318 the melanomas (SKCM, UVM) and squamous cell cancers (BLCA, CECS, HNSC, LUSC, and
319 some ESCA) forming distinct clusters. The core gastrointestinal tract cancers cluster tightly, with
320 COAD and READ embedded into an inseparable mass which is adjoined by STAD and some
321 ESCA samples. ESCA samples clearly segregate into two populations, consistent with both
322 esophageal adenocarcinoma (clustered with STAD) and squamous cell carcinoma (clustered
323 with LUSC, HNSC, etc.) being classified under ESCA (Zheng 2013). Similarly, the known
324 similarities between USC, UCEC, and SARC clearly emerges, with the embedding of USC
325 forming a bridge between UCEC and SARC clusters; we also observe two distinct clusters of
326 SARC samples, one most similar to USC and the other most similar to UCEC. As this
327 embedding is heavily dependent on the input samples and number thereof, it may be that some
328 misclassifications are unavoidable without a larger cohort of samples.
329

330 **3.1.1 Cancer type classifier performed well on external expression data**

331 To further validate the primary type classifier, we classified 1,552 samples across 9 primary
332 tumor types (Figure 4A) profiled using microarrays from the Expression Project for Oncology
333 (expO, GSE2109 [35]). Due to the age of the dataset, primary cancer types corresponding to
334 the brain (LGG, GBM), lung (LUAD, LUSC), and kidney (KIRC, KIRP, KIRH) were aggregated to
335 match the respective primary tumor annotations of the dataset. Further, the genes used for
336 classification were reduced to 1,788 genes from the initially selected genes of 1,971 in order to
337 match those found in the external dataset, and the model was retrained on the training set with
338 only these 1,788 features. This external validation set not only tests the classifier performance
339 independent of batch variation, but also its independence of the platform and robustness to

340 feature loss which are critical for the application of the classifiers in clinical and translational
341 research.
342
343 Classification by primary cancer types, shown in Figure 4B, yields specificity of 99.3% and
344 median sensitivity of 78.1% (n=9) (Figure 4C), with misclassifications largely within organ
345 systems. For example, misclassification arises between gastrointestinal cancers STAD, COAD,
346 and LIHC, and ovarian serous cystadenocarcinoma (OV) is misclassified as cancers with similar
347 histology or anatomical location. When the classification is reorganized by pan-organ group, as
348 shown in Figure 4D, median sensitivity increases to 86.0% (n=6) with the misclassification only
349 between core and developmental gastrointestinal cancers (Figure 4E).
350
351 **3.1.2 Classifier can identify cancer of unknown primary**
352 Identification of the primary cancer (tissue) of origin from a metastatic sample is a significant
353 clinical challenge. As metastases are expected to retain the transcriptional signature of primary
354 tumor of origin, we hypothesize that our classifier can identify the primary tumor type from
355 metastatic samples. We examined the performance of our classifiers using an external
356 validating dataset from metastatic tumors.
357
358 Primary type classification of expression profiles of 88 metastatic samples across 6 known
359 primary types is shown in Figure 5A,B [36]. The median specificity is 99.3%, and the median
360 sensitivity is 82.1%. The most common misclassifications were, again, between COAD and
361 STAD, the vast majority involving metastatic tumors in the liver. Within-organ-system
362 classification (Figure 5C) shows the minimum sensitivity substantially improves from 20.0% to
363 69.0%, where predictions of these gastrointestinal cancers are combined (Figure 5D). Further
364 examination revealed that the most common metastases in the data, 30/88 (34%) samples, are
365 to the liver or lung from the colon, illustrated in Figure 5E. Of the 88 tumors, 52 metastases

366 (59.1%) are classified to the correct primary tumor type, 72 metastases (81.8%) are classified to
367 the correct primary organ system, 7 metastases (7.9%) are classified as the tumor from the
368 respective metastasized sites, and 9 metastases (10.1%) are classified incorrectly (Figure 5F)
369 i.e. neither as tumor of primary site nor as the metastasized site.
370
371 We further validate our classifiers independently using an external dataset from patient-derived
372 xenograft (PDX) models of cancer. PDX models of cancer are a great resource to evaluate
373 therapeutic regimens but can also be used as a tool to study metastatic cancer, as illustrated in
374 Figure 6A. Primary tumor is resected from human patients and tumor fragments are implanted
375 into a cohort of immunodeficient mice [63]. After a growth period, the mouse-grown tumor is
376 resected and implanted into a new generation of mice. This process can be repeated several
377 times.
378
379 We performed the primary tumor type classification of 318 PDX-derived mouse-grown tumors
380 (samples were taken from the second generation of mice) spanning 11 cancer types (Figure 6B-
381 C). Classification of primary cancer types yields a median specificity of 99.5% (n=11), and
382 median sensitivity of 76% (n=11) (Figure 6D). When classified by pan-organ system, the median
383 sensitivity increases to 83% (Figure 6E,F). Despite not being present in the set of primary
384 cancers, several tumors including COAD and PAAD are classified as STAD, possibly due to the
385 close proximity of anatomic positions.
386
387 These three external validations of our model overwhelmingly support the hypothesis that
388 metastatic and xenograft tumors retain the molecular signature of the primary
389 tumor. Application of such models in the clinic will allow for more effective treatments of CUPs.
390
391 **3.2 Subtype specific classification accurately identifies molecular subtypes**

392 Molecular subtypes have been defined for 11 cancer types: BRCA, HNSC, KIRC, KIRP, LGG,
393 LUAD, LUSC, OV, PRAD, SKCM, and STAD. Each of these primary types has two to four
394 molecular subtypes. For example, breast cancers are frequently subtyped into Basal-like, Her2-
395 enriched, Luminal A and Luminal B. This subtyping has prognostic power and can be used as
396 predictive marker for therapeutic approaches [64].
397
398 Eleven models were constructed, one model for each primary tumor type, into its molecular
399 subtypes, as illustrated schematically in Figure 1. The positive predictive value, sensitivity,
400 specificity, and number of samples per subtype are shown in Figure 7A-D. The best performing
401 subtype classifiers, LGG, LUAD, PRAD, have median sensitivity above 90%, with PRAD
402 yielding nearly perfect classification.
403
404 **3.2.1 Subtype classifiers are accurate on external data of different platforms**
405 To further validate the cancer subtype classifiers, we classified samples from two external
406 datasets: ovarian cancer [15] and breast cancer [38] annotated with molecular subtypes, with
407 215 and 1,784 samples respectively. The ovarian cancer subtype classifier (Figure 7E,F)
408 reached a median specificity of 94.9% (the best performance is for mesenchymal: 99.2%) and a
409 median sensitivity of 88.4% (the best performance is proliferative: 97.2%). The breast cancer
410 subtype classifier, shown in Figure 7G,H, presented a median specificity of 95% (the best
411 performance is for basal-like: 99.9%) and a median sensitivity of 72.4% (the best performance is
412 for luminal-A subtype: 95%). Notably, the basal-like molecular subtype of breast cancer is a
413 particularly aggressive subtype and patients relapse rapidly. The accurate classification of this
414 subtype is important for precise treatment—recently, a diabetes drug has been shown as a
415 potential therapy for basal-like breast cancer patients [65]. The two external validation datasets
416 from 1,999 patients with breast or ovarian cancers demonstrate that our subtype classifier can
417 distinguish clinically favorable subtypes from those associated with poor prognosis.

418

419 Together with the identification of primary origin for metastatic tumors, followed by subtype
420 classification together allows for informed therapeutic decision making for clinicians, thereby
421 improving treatment outcomes for CUP patients.

422

423 **4. DISCUSSION**

424 It is widely appreciated that cancer is a disease at the scale of the entire genome, but it remains
425 difficult to effectively translate this complexity into clinical utilities. Two important pieces of
426 information that are relevant in clinical care and translational research are knowledge of tissue
427 of origin, or CUP, and subtype of the cancer. Identifying tissue of origin of CUPs and molecular
428 subtype is critical for personalized medicine, where the treatment is tailored to the molecular
429 profile of individual tumor [66]. Because of the lack of primary site information, CUP patients
430 receive palliative chemotherapy that lacks the precision of modern targeted cancer medicine
431 and results in no clear benefit in survival [67, 68]. Various approved targeted therapies for
432 cancer by the Food and Drug Administration (FDA) include signal transduction inhibitors, gene
433 expression modulators, apoptosis inducers, angiogenesis inhibitors, immunotherapies. The
434 targeted therapies have been approved for the treatment of over 28 types of cancer. As CUP
435 may retain molecular signatures of its primary site, CUP patients with primary or metastatic
436 tumor might benefit from established therapeutic regimens appropriate for cancers of that
437 tissue; therefore, identifying the primary site is key to choosing effective therapeutic options.

438

439 Another major challenge in clinical cancer research is accurately classifying cancers into
440 appropriate homogeneous subtypes to improve prognosis and treatment [5]. Analyses of The
441 Cancer Genome Atlas (TCGA) and the International Cancer Genome Consortium (ICGC) have
442 established that a cancer at any primary site can be further classified into molecular subtypes

443 with potentially distinct clinical outcome and therapeutic options [21-28, 62]. For example, the
444 EBV-positive subtype of gastric cancer is associated with overexpression of JAK2, PD-L1 and
445 PD-L2 genes, suggesting that PD-L1/2 antagonists and JAK2 inhibitors are potential therapeutic
446 options for these tumors [64]. Similar clinical and therapeutic relevance of subtype information
447 has been demonstrated in multiple cancers [21, 23-25, 27, 28]. Increasingly, tumor molecular
448 subtype is being considered as an eligibility criterion for the entry into clinical trials [29].
449 However, for many cancers, the molecular subtype information is not available for use in clinical
450 practice because of the difficulty in identifying the subtype of a given tumor [30, 31]. Besides
451 being an important factor in clinical decision making, the knowledge of the molecular subtype
452 will be helpful in translational research. For example, cancer avatar trials use PDX models to
453 test panels of drugs to determine the best regime for personalized human therapy. Knowledge
454 of subtype of the tumor may narrow down the choice of treatment regimens to test which
455 increases efficiency of the cancer avatar trials.

456

457 We developed classifiers of high sensitivity and specificity for prediction of tissue of origin of 33
458 cancers and molecular subtyping of 11 cancers using gene expression data from the TCGA. We
459 show, for the first time to our knowledge, our pan-cancer classifiers can predict multiple cancers'
460 primary of origin from metastatic samples. Compared to the other classifiers based on somatic
461 mutations [69], our classifier is not limited to only cancer types with high mutation burden and
462 has much greater potential for clinical diagnosis and therapeutic design. Further, the classifiers
463 trained on the TCGA RNA-seq data generalize to different cohorts of primary and metastatic
464 samples profiled using microarray sequencing technologies. Such external validation qualifies
465 our classifiers to be robust across technology platforms, batches and sample processing
466 protocols. A combination of primary tissue of origin and subtype classification from metastases
467 will serve as important tools for clinicians in effectively treating CUPs.

468

469 The classification tools discriminated all cancers from each other well, except among the gastro-
470 intestinal cancers. However, the classification by cancer group could be achieved with very high
471 sensitivity and specificity. Different cancers among gastrointestinal cancers are less
472 distinguishable due to their anatomic proximity and molecular similarity, as shown in Figure 3.
473 To circumvent this problem, in our future work, we will adopt a hierarchical classification of
474 tumors: (1) granular classification by cancer group (2) finer classification by cancer type in each
475 group. In addition, we can include features from copy number, mutation and methylation data to
476 augment our feature set for both accuracy as well as robustness for technology and batch
477 variations. Molecular subtyping can also benefit from adding features from heterogeneous data
478 as several subtypes were identified to exhibit genomic features that span whole spectrum of
479 omics data. For example, the CIN subtype in gastric cancer is known to exhibit large structural
480 variations which may not be captured accurately by expression data. Thus, our future work will
481 encompass comprehensive multi-omic data to identify tissue of origin and molecular subtyping.
482

483 Though the overall performance of the classifiers designed using DLDA, SVM and KNN is not
484 as good as Random Forest on this data, their performance is on par with or better than Random
485 Forest based classifiers on certain tumor type and subtype classification. However, the
486 classification predicted by Random Forest classifiers is easier to interpret.
487

488 As we continue to enhance the classifier, we do recognize that the clinical utility of the classifier
489 is dependent on its ability to classify FFPE (formalin-fixed paraffin-embedded) samples, which is
490 the standard specimen type used for molecular profiling of cancers in clinical diagnostics in
491 addition to fresh-frozen samples. We have previously shown that the classifiers designed can
492 work with FFPE samples if they are profiled using nanoString arrays [70]. Therefore, it is
493 feasible to generalize our classifiers to work on FFPE samples for clinical applications. In

494 summary, we have demonstrated the utility of gene expression profiles to solve the important
495 clinical challenge of identifying the primary site of origin and the molecular subtype of cancers
496 based on machine learning algorithms. These predictors will be made available as open source
497 software, freely available for academic non-commercial use.

498

499 In an effort make these tools available to as wide an audience as possible, we offer our models
500 and results in two publicly available forms: a web-based portal and a software package which
501 can be used to apply these tools to other datasets and to reproduce the results presented
502 here. The web-based portal provides interactive visualizations showing the expression profiles
503 of the TCGA cancer samples and the classification results of our classifiers. These
504 visualizations allow for the exploration of relationships between cancer types in the context of
505 pan-cancer expression profiles.

506

507 **SUPPORTING INFORMATION**

508 Table S1. Contingency table and all performance metrics – random forest
509 Table S2. Contingency table and all performance metrics – SVM
510 Table S3. Contingency table and all performance metrics – kNN
511 Table S4. Contingency table and all performance metrics – DLDA
512 Table S5. Performance metrics for external datasets – random forest

513

514 **ACKNOWLEDGEMENTS**

515 Research reported in this publication was partially supported by the National Cancer Institute of
516 the National Institutes of Health under Award Number P30CA034196. The content is solely the
517 responsibility of the authors and does not necessarily represent the official views of the National
518 Institutes of Health. This study makes use of data generated by the Molecular Taxonomy of

Breast Cancer International Consortium. Funding for the project was provided by Cancer Research UK and the British Columbia Cancer Agency Branch.

AUTHOR CONTRIBUTIONS

R.K.M.K. and J.G. designed research. S.L., R.K.M.K. and J.G. guided the project. C.A.P. and J.G. performed data acquisition. W.F.F. and J.G. wrote software and performed analysis. H.R. provided input on clinical oncology and contributed to the interpretation of the results. S.N. provided computational support. W.F.F., S.N., C.A.P., H.R., S.L., R.K.M.K., J.G. wrote the manuscript.

529 **FIGURE LEGENDS**

530 **Figure 1. Platform-independent learning and validation from TCGA transcriptomes.**
531 (A) Schematic showing the learning procedure used to train machine learning models from
532 labeled TCGA transcriptomes spanning 33 cancer types and 11 molecular subtypes. Models
533 were trained and evaluated using k-fold cross validation on normalized and standard scaled
534 expression profiles. For each fold, N features were selected from each class (see Methods) and
535 pooled, which were used to train the classification model. Using this schema, we constructed
536 one primary type and eleven molecular subtype classifiers for each type of model: random
537 forest (RF), support vector machine (SVM), k-nearest neighbor classifier (kNN), and diagonal
538 linear discriminant analysis (DLDA). (B) Classification performance was evaluated via the
539 cross-validation on the learning set and external validation utilizing five datasets; using two of
540 these datasets, we challenged the classifier to infer primary tumor types from transcriptomes of
541 metastatic or passaged patient-derived xenograft samples.

542

543 **Figure 2. Precise classification of tumors by primary type and organ system.**
544 (A-B) Random forest classification of primary cancer types and grouped by pan-organ system.
545 Text in contingency table cell $c_{j,i}$ shows tumor of class *i* classified as class *j*. Grayscale shading
546 of table cells is proportional to the number of samples of each tumor type, represented as bars
547 above the table. Color shading along the main diagonal shows pan-organ groups. Positive
548 predictive value (precision) for each prediction class are shown to the right of the table. (C-D)
549 Sensitivity and specificity for each classification in (A) and (B), respectively.

550

551 **Figure 3. Unsupervised embedding of expression profiles reveals relationships among**
552 **primary cancer types.**
553 Expression profiles from all samples were embedded into two dimensions using uniform
554 manifold approximation and projection (UMAP) [58] and colored by primary cancer type. For

555 each cancer, labels are placed near the centroid of the expression profile in the UMAP latent
556 space. Anatomical and histological relationships are emergent and add context to the most
557 common misclassifications in Figure 2. The following groups of cancers are highlighted with
558 green, blue, and purple ellipses, respectively: COAD, READ, STAD; BLCA, CESC, ESCA,
559 HNSC, LUSC; OV, SARC, UCEC, UCS.
560
561 **Figure 4. External validation of primary type classifier using microarray data.**
562 1,552 microarray expression profiles (GSE2109) from 9 cancer types or related cancer types
563 (LUSC/LUAD and KIRC/KIRP/KICH) were classified to further validate the primary type
564 classifier (A). Markers in (A) are scaled by the number of samples in each class. Classification
565 was evaluated by primary cancer type (B) and pan-organ group (C). (D-E) Sensitivity and
566 specificity for each classification in (B) and (C), respectively.
567
568 **Figure 5. Classifier infers primary cancer of origin from metastatic tumor samples.**
569 (A-B) 88 expression profiles of metastatic tumors (GSE18549) from primary cancers of origin
570 spanning 6 organs were classified by primary cancer type and primary pan-organ group. (C-D)
571 Sensitivity and specificity for each classification in (A) and (B), respectively. (E) 30/88 (34%) of
572 samples are liver or lung metastases from the colon. (F) The majority of misclassifications of
573 primary type are within pan-organ system; of the remainder, 7 misclassifications identify the
574 metastatic tumor whereas 9 are true misclassifications.
575
576 **Figure 6. Classifier infers primary cancer of origin from passaged patient-derived**
577 **xenografts.**
578 (A) 295 expression profiles of resected passaged patient-derived xenograft (PDX) tumors from
579 primary cancers spanning 11 organs were classified by primary cancer type (samples generated
580 at the Jackson Laboratory, available via MTB [37]). PDX tumor samples were taken for

581 sequencing from the second generation of mice. Classification of primary cancer identification
582 was evaluated by primary cancer type (B) and pan-organ group (C). (D-E) Sensitivity and
583 specificity for each classification in (B) and (C), respectively.
584
585 **Figure 7. Cross- and external validation of molecular subtype classifiers.**
586 A classifier of molecular subtypes was constructed for each of 11 primary cancer types,
587 spanning 38 molecular subtypes. (A) Per-class positive predictive value, (B) specificity, and (C)
588 sensitivity of molecular subtype classifications evaluated through cross-validation (Figure 1).
589 (D) Number of training samples for each molecular subtype. To further validate these subtype
590 classifiers, breast (E) and ovarian (F) subtype classifiers were used to predict the respective
591 molecular subtypes in two external datasets (GSE9899 and EGAS00000000083, respectively).
592 (G-H) Sensitivity and specificity for each classification in (E) and (F), respectively.
593

REFERENCES

1. Pavlidis N, Khaled H, Gaafar R. A mini review on cancer of unknown primary site: A clinical puzzle for the oncologists. J Adv Res. 2015;6(3):375-82. Epub 2015/08/11. doi: 10.1016/j.jare.2014.11.007. PubMed PMID: 26257935; PubMed Central PMCID: PMC4522587.
2. Moran S, Martinez-Cardus A, Boussios S, Esteller M. Precision medicine based on epigenomics: the paradigm of carcinoma of unknown primary. Nat Rev Clin Oncol. 2017;14(11):682-94. Epub 2017/07/05. doi: 10.1038/nrclinonc.2017.97. PubMed PMID: 28675165.
3. Hyphantis T, Papadimitriou I, Petrakis D, Fountzilas G, Repana D, Assimakopoulos K, et al. Psychiatric manifestations, personality traits and health-related quality of life in cancer of unknown primary site. Psychooncology. 2013;22(9):2009-15. Epub 2013/01/30. doi: 10.1002/pon.3244. PubMed PMID: 23359412.
4. Hainsworth JD, Schnabel CA, Erlander MG, Haines DW, 3rd, Greco FA. A retrospective study of treatment outcomes in patients with carcinoma of unknown primary site and a colorectal cancer molecular profile. Clin Colorectal Cancer. 2012;11(2):112-8. Epub 2011/10/18. doi: 10.1016/j.clcc.2011.08.001. PubMed PMID: 22000811.
5. Varadhachary GR, Talantov D, Raber MN, Meng C, Hess KR, Jatkoe T, et al. Molecular profiling of carcinoma of unknown primary and correlation with clinical evaluation. J Clin Oncol. 2008;26(27):4442-8. Epub 2008/09/20. doi: 10.1200/JCO.2007.14.4378. PubMed PMID: 18802157.
6. Yoon HH, Foster NR, Meyers JP, Steen PD, Visscher DW, Pillai R, et al. Gene expression profiling identifies responsive patients with cancer of unknown primary treated with carboplatin, paclitaxel, and everolimus: NCCTG N0871 (alliance). Ann Oncol. 2016;27(2):339-44. Epub 2015/11/19. doi: 10.1093/annonc/mdv543. PubMed PMID: 26578722; PubMed Central PMCID: PMC4907341.
7. Varadhachary GR, Spector Y, Abbruzzese JL, Rosenwald S, Wang H, Aharonov R, et al. Prospective gene signature study using microRNA to identify the tissue of origin in patients with carcinoma of unknown primary. Clin Cancer Res. 2011;17(12):4063-70. Epub 2011/05/03. doi: 10.1158/1078-0432.CCR-10-2599. PubMed PMID: 21531815.
8. Hainsworth JD, Rubin MS, Spigel DR, Boccia RV, Raby S, Quinn R, et al. Molecular gene expression profiling to predict the tissue of origin and direct site-specific therapy in patients with carcinoma of unknown primary site: a prospective trial of the Sarah Cannon research institute. J Clin Oncol. 2013;31(2):217-23. Epub 2012/10/04. doi: 10.1200/JCO.2012.43.3755. PubMed PMID: 23032625.
9. Varadhachary GR, Karanth S, Qiao W, Carlson HR, Raber MN, Hainsworth JD, et al. Carcinoma of unknown primary with gastrointestinal profile: immunohistochemistry and survival data for this favorable subset. Int J Clin Oncol. 2014;19(3):479-84. Epub 2013/07/03. doi: 10.1007/s10147-013-0583-0. PubMed PMID: 23813044.
10. Green AC. Cancer of unknown primary: does the key lie in molecular diagnostics? Cytopathology. 2015;26(1):61-3. Epub 2015/02/17. doi: 10.1111/cyt.12235. PubMed PMID: 25683360.
11. Kandalaft PL, Gown AM. Practical Applications in Immunohistochemistry: Carcinomas of Unknown Primary Site. Arch Pathol Lab Med. 2016;140(6):508-23. Epub 2015/10/13. doi: 10.5858/arpa.2015-0173-CP. PubMed PMID: 26457625.
12. Conner JR, Hornick JL. Metastatic carcinoma of unknown primary: diagnostic approach using immunohistochemistry. Adv Anat Pathol. 2015;22(3):149-67. Epub 2015/04/07. doi: 10.1097/PAP.0000000000000069. PubMed PMID: 25844674.
13. Rubin BP, Skarin AT, Pisick E, Rizk M, Salgia R. Use of cytokeratins 7 and 20 in determining the origin of metastatic carcinoma of unknown primary, with special emphasis on lung cancer. Eur J Cancer Prev. 2001;10(1):77-82. Epub 2001/03/27. PubMed PMID: 11263595.

645 14. Gunia S, Koch S, May M. Is CDX2 immunostaining useful for delineating anorectal from
646 penile/vulvar squamous cancer in the setting of squamous cell carcinoma with clinically unknown
647 primary site presenting with histologically confirmed inguinal lymph node metastasis? J Clin
648 Pathol. 2013;66(2):109-12. Epub 2012/10/30. doi: 10.1136/jclinpath-2012-201138. PubMed
649 PMID: 23105122.
650 15. Tothill RW, Kowalczyk A, Rischin D, Bousioutas A, Haviv I, van Laar RK, et al. An
651 expression-based site of origin diagnostic method designed for clinical application to cancer of
652 unknown origin. Cancer Res. 2005;65(10):4031-40. Epub 2005/05/19. doi: 10.1158/0008-
653 5472.CAN-04-3617. PubMed PMID: 15899792.
654 16. Horlings HM, van Laar RK, Kerst JM, Helgason HH, Wesseling J, van der Hoeven JJ, et
655 al. Gene expression profiling to identify the histogenetic origin of metastatic adenocarcinomas of
656 unknown primary. J Clin Oncol. 2008;26(27):4435-41. Epub 2008/09/20. doi:
657 10.1200/JCO.2007.14.6969. PubMed PMID: 18802156.
658 17. Varadhachary GR, Raber MN, Matamoros A, Abbruzzese JL. Carcinoma of unknown
659 primary with a colon-cancer profile-changing paradigm and emerging definitions. Lancet Oncol.
660 2008;9(6):596-9. Epub 2008/05/31. doi: 10.1016/S1470-2045(08)70151-7. PubMed PMID:
661 18510991.
662 18. van Laar RK, Ma XJ, de Jong D, Wehkamp D, Floore AN, Warmoes MO, et al.
663 Implementation of a novel microarray-based diagnostic test for cancer of unknown primary. Int J
664 Cancer. 2009;125(6):1390-7. Epub 2009/06/19. doi: 10.1002/ijc.24504. PubMed PMID:
665 19536816.
666 19. Handorf CR, Kulkarni A, Grenert JP, Weiss LM, Rogers WM, Kim OS, et al. A multicenter
667 study directly comparing the diagnostic accuracy of gene expression profiling and
668 immunohistochemistry for primary site identification in metastatic tumors. Am J Surg Pathol.
669 2013;37(7):1067-75. Epub 2013/05/08. doi: 10.1097/PAS.0b013e31828309c4. PubMed PMID:
670 23648464; PubMed Central PMCID: PMC5266589.
671 20. Greco FA, Lennington WJ, Spigel DR, Hainsworth JD. Molecular profiling diagnosis in
672 unknown primary cancer: accuracy and ability to complement standard pathology. J Natl Cancer
673 Inst. 2013;105(11):782-90. Epub 2013/05/04. doi: 10.1093/jnci/djt099. PubMed PMID: 23641043.
674 21. Cancer Genome Atlas N. Comprehensive molecular portraits of human breast tumours.
675 Nature. 2012;490(7418):61-70. Epub 2012/09/25. doi: 10.1038/nature11412. PubMed PMID:
676 23000897; PubMed Central PMCID: PMC3465532.
677 22. Cancer Genome Atlas N. Comprehensive genomic characterization of head and neck
678 squamous cell carcinomas. Nature. 2015;517(7536):576-82. Epub 2015/01/30. doi:
679 10.1038/nature14129. PubMed PMID: 25631445; PubMed Central PMCID: PMC4311405.
680 23. Cancer Genome Atlas N. Comprehensive molecular characterization of human colon and
681 rectal cancer. Nature. 2012;487(7407):330-7. Epub 2012/07/20. doi: 10.1038/nature11252.
682 PubMed PMID: 22810696; PubMed Central PMCID: PMC3401966.
683 24. Cancer Genome Atlas Research N. Comprehensive genomic characterization defines
684 human glioblastoma genes and core pathways. Nature. 2008;455(7216):1061-8. Epub
685 2008/09/06. doi: 10.1038/nature07385. PubMed PMID: 18772890; PubMed Central PMCID:
686 PMC2671642.
687 25. Cancer Genome Atlas Research N. Integrated genomic analyses of ovarian carcinoma.
688 Nature. 2011;474(7353):609-15. Epub 2011/07/02. doi: 10.1038/nature10166. PubMed PMID:
689 21720365; PubMed Central PMCID: PMC3163504.
690 26. Cancer Genome Atlas Research N. Comprehensive genomic characterization of
691 squamous cell lung cancers. Nature. 2012;489(7417):519-25. Epub 2012/09/11. doi:
692 10.1038/nature11404. PubMed PMID: 22960745; PubMed Central PMCID: PMC3466113.
693 27. Cancer Genome Atlas Research N. Comprehensive molecular profiling of lung
694 adenocarcinoma. Nature. 2014;511(7511):543-50. Epub 2014/08/01. doi: 10.1038/nature13385.
695 PubMed PMID: 25079552; PubMed Central PMCID: PMC4231481.

696 28. Cancer Genome Atlas Research N. The Molecular Taxonomy of Primary Prostate Cancer.
697 Cell. 2015;163(4):1011-25. Epub 2015/11/07. doi: 10.1016/j.cell.2015.10.025. PubMed PMID:
698 26544944; PubMed Central PMCID: PMC4695400.
699 29. Kommoss S, Winterhoff B, Oberg AL, Konecny GE, Wang C, Riska SM, et al.
700 Bevacizumab May Differentially Improve Ovarian Cancer Outcome in Patients with Proliferative
701 and Mesenchymal Molecular Subtypes. Clin Cancer Res. 2017;23(14):3794-801. Epub
702 2017/02/06. doi: 10.1158/1078-0432.CCR-16-2196. PubMed PMID: 28159814; PubMed Central
703 PMCID: PMC5661884.
704 30. Prat A, Fan C, Fernandez A, Hoadley KA, Martinello R, Vidal M, et al. Response and
705 survival of breast cancer intrinsic subtypes following multi-agent neoadjuvant chemotherapy.
706 BMC Med. 2015;13:303. Epub 2015/12/20. doi: 10.1186/s12916-015-0540-z. PubMed PMID:
707 26684470; PubMed Central PMCID: PMC4683815.
708 31. Prat A, Pineda E, Adamo B, Galvan P, Fernandez A, Gaba L, et al. Clinical implications
709 of the intrinsic molecular subtypes of breast cancer. Breast. 2015;24 Suppl 2:S26-35. Epub
710 2015/08/09. doi: 10.1016/j.breast.2015.07.008. PubMed PMID: 26253814.
711 32. Li B, Dewey CN. RSEM: accurate transcript quantification from RNA-Seq data with or
712 without a reference genome. BMC Bioinformatics. 2011;12(1). doi: 10.1186/1471-2105-12-323.
713 33. Center BITGDA. Analysis-ready standardized TCGA data from Broad GDAC Firehose
714 2016_01_28 run. Broad Institute of MIT and Harvard: Broad Institute of MIT and Harvard; 2016.
715 34. Huber W, Carey VJ, Gentleman R, Anders S, Carlson M, Carvalho BS, et al. Orchestrating
716 high-throughput genomic analysis with Bioconductor. Nat Methods. 2015;12(2):115-21. Epub
717 2015/01/31. doi: 10.1038/nmeth.3252. PubMed PMID: 25633503; PubMed Central PMCID:
718 PMC4509590.
719 35. Singh R, Maganti RJ, Jabba SV, Wang M, Deng G, Heath JD, et al. Microarray-based
720 comparison of three amplification methods for nanogram amounts of total RNA. American Journal
721 of Physiology-Cell Physiology. 2005;288(5):C1179-C89. doi: 10.1152/ajpcell.00258.2004.
722 36. Hsu SD, Kim MK, Foye A, Silvestri A, Lyerly HK, Morse M, et al. Use of gene expression
723 signatures to identify origin of primary and therapeutic strategies for patients with advanced solid
724 tumors. Journal of Clinical Oncology. 2010;28(15_suppl):10504-. doi:
725 10.1200/jco.2010.28.15_suppl.10504.
726 37. Krupke DM, Begley DA, Sundberg JP, Bult CJ, Eppig JT. The Mouse Tumor Biology
727 database. Nat Rev Cancer. 2008;8(6):459-65. Epub 2008/04/25. doi: 10.1038/nrc2390. PubMed
728 PMID: 18432250; PubMed Central PMCID: PMC2574871.
729 38. Curtis C, Shah SP, Chin SF, Turashvili G, Rueda OM, Dunning MJ, et al. The genomic
730 and transcriptomic architecture of 2,000 breast tumours reveals novel subgroups. Nature.
731 2012;486(7403):346-52. Epub 2012/04/24. doi: 10.1038/nature10983. PubMed PMID: 22522925;
732 PubMed Central PMCID: PMC3440846.
733 39. Cerami E, Gao J, Dogrusoz U, Gross BE, Sumer SO, Aksoy BA, et al. The cBio cancer
734 genomics portal: an open platform for exploring multidimensional cancer genomics data. Cancer
735 Discov. 2012;2(5):401-4. Epub 2012/05/17. doi: 10.1158/2159-8290.CD-12-0095. PubMed PMID:
736 22588877; PubMed Central PMCID: PMC3956037.
737 40. Gao J, Aksoy BA, Dogrusoz U, Dresdner G, Gross B, Sumer SO, et al. Integrative analysis
738 of complex cancer genomics and clinical profiles using the cBioPortal. Sci Signal.
739 2013;6(269):pl1. Epub 2013/04/04. doi: 10.1126/scisignal.2004088. PubMed PMID: 23550210;
740 PubMed Central PMCID: PMC4160307.
741 41. Ceccarelli M, Barthel FP, Malta TM, Sabedot TS, Salama SR, Murray BA, et al. Molecular
742 Profiling Reveals Biologically Discrete Subsets and Pathways of Progression in Diffuse Glioma.
743 Cell. 2016;164(3):550-63. Epub 2016/01/30. doi: 10.1016/j.cell.2015.12.028. PubMed PMID:
744 26824661; PubMed Central PMCID: PMC4754110.

42. Getz G, Gabriel SB, Cibulskis K, Lander E, Sivachenko A, Sougnez C, et al. Integrated genomic characterization of endometrial carcinoma. Nature. 2013;497(7447):67-73. doi: 10.1038/nature12113.
43. Akbani R, Akdemir Kadir C, Aksoy BA, Albert M, Ally A, Amin Samirkumar B, et al. Genomic Classification of Cutaneous Melanoma. Cell. 2015;161(7):1681-96. doi: 10.1016/j.cell.2015.05.044.
44. Comprehensive Molecular Characterization of Papillary Renal-Cell Carcinoma. New England Journal of Medicine. 2016;374(2):135-45. doi: 10.1056/NEJMoa1505917.
45. Comprehensive molecular characterization of clear cell renal cell carcinoma. Nature. 2013;499(7456):43-9. doi: 10.1038/nature12222.
46. Hoadley KA, Yau C, Hinoue T, Wolf DM, Lazar AJ, Drill E, et al. Cell-of-Origin Patterns Dominate the Molecular Classification of 10,000 Tumors from 33 Types of Cancer. Cell. 2018;173(2):291-304 e6. Epub 2018/04/07. doi: 10.1016/j.cell.2018.03.022. PubMed PMID: 29625048; PubMed Central PMCID: PMC5957518.
47. Dudoit S, Fridlyand J, Speed TP. Comparison of Discrimination Methods for the Classification of Tumors Using Gene Expression Data. Journal of the American Statistical Association. 2002;97(457):77-87. doi: 10.1198/016214502753479248.
48. Tabchy A, Valero V, Vidaurre T, Lluch A, Gomez H, Martin M, et al. Evaluation of a 30-gene paclitaxel, fluorouracil, doxorubicin, and cyclophosphamide chemotherapy response predictor in a multicenter randomized trial in breast cancer. Clin Cancer Res. 2010;16(21):5351-61. Epub 2010/09/11. doi: 10.1158/1078-0432.CCR-10-1265. PubMed PMID: 20829329; PubMed Central PMCID: PMC4181852.
49. Kurokawa C, Iankov ID, Anderson SK, Aderca I, Leontovich AA, Maurer MJ, et al. Constitutive Interferon Pathway Activation in Tumors as an Efficacy Determinant Following Oncolytic Virotherapy. J Natl Cancer Inst. 2018. Epub 2018/05/23. doi: 10.1093/jnci/djy033. PubMed PMID: 29788332.
50. Khondoker M, Dobson R, Skirrow C, Simmons A, Stahl D. A comparison of machine learning methods for classification using simulation with multiple real data examples from mental health studies. Stat Methods Med Res. 2016;25(5):1804-23. Epub 2013/09/21. doi: 10.1177/0962280213502437. PubMed PMID: 24047600; PubMed Central PMCID: PMC5081132.
51. Li Y, Kang K, Krahn JM, Croutwater N, Lee K, Umbach DM, et al. A comprehensive genomic pan-cancer classification using The Cancer Genome Atlas gene expression data. BMC Genomics. 2017;18(1):508. Epub 2017/07/05. doi: 10.1186/s12864-017-3906-0. PubMed PMID: 28673244; PubMed Central PMCID: PMC5496318.
52. Li Z, Mao Y, Li H, Yu G, Wan H, Li B. Differentiating brain metastases from different pathological types of lung cancers using texture analysis of T1 postcontrast MR. Magn Reson Med. 2016;76(5):1410-9. Epub 2015/12/02. doi: 10.1002/mrm.26029. PubMed PMID: 26621795.
53. Venables WN, Ripley BD. Modern Applied Statistics with S2002.
54. Wang S, Cai Y. Identification of the functional alteration signatures across different cancer types with support vector machine and feature analysis. Biochim Biophys Acta. 2018;1864(6 Pt B):2218-27. Epub 2017/12/27. doi: 10.1016/j.bbadis.2017.12.026. PubMed PMID: 29277326.
55. Galvez JM, Castillo D, Herrera LJ, San Roman B, Valenzuela O, Ortuno FM, et al. Multiclass classification for skin cancer profiling based on the integration of heterogeneous gene expression series. PLoS One. 2018;13(5):e0196836. Epub 2018/05/12. doi: 10.1371/journal.pone.0196836. PubMed PMID: 29750795; PubMed Central PMCID: PMC5947894.
56. Zhi J, Sun J, Wang Z, Ding W. Support vector machine classifier for prediction of the metastasis of colorectal cancer. Int J Mol Med. 2018;41(3):1419-26. Epub 2018/01/13. doi: 10.3892/ijmm.2018.3359. PubMed PMID: 29328363; PubMed Central PMCID: PMC5819940.

57. Breiman L. Consistency for a simple model of random forests. Univ. California, Berkeley, CA: 2004 Contract No.: Technical Report 670.
58. McInnes L, Healy J. UMAP: Uniform Manifold Approximation and Projection for Dimension Reduction. ArXiv e-prints [Internet]. 2018.
59. van der Maaten L. Accelerating t-SNE using Tree-Based Algorithms. Journal of Machine Learning Research. 2014;15:3221-45.
60. Ulyanov D. Multicore-TSNE. GitHub; 2016.
61. Zhang Y. Epidemiology of esophageal cancer. World J Gastroenterol. 2013;19(34):5598-606. Epub 2013/09/17. doi: 10.3748/wjg.v19.i34.5598. PubMed PMID: 24039351; PubMed Central PMCID: PMC3769895.
62. Cherniack AD, Shen H, Walter V, Stewart C, Murray BA, Bowlby R, et al. Integrated Molecular Characterization of Uterine Carcinosarcoma. Cancer Cell. 2017;31(3):411-23. Epub 2017/03/16. doi: 10.1016/j.ccell.2017.02.010. PubMed PMID: 28292439; PubMed Central PMCID: PMC5599133.
63. Hidalgo M, Amant F, Biankin AV, Budinska E, Byrne AT, Caldas C, et al. Patient-derived xenograft models: an emerging platform for translational cancer research. Cancer Discov. 2014;4(9):998-1013. Epub 2014/09/04. doi: 10.1158/2159-8290.CD-14-0001. PubMed PMID: 25185190; PubMed Central PMCID: PMC4167608.
64. Bass AJ, Thorsson V, Shmulevich I, Reynolds SM, Miller M, Bernard B, et al. Comprehensive molecular characterization of gastric adenocarcinoma. Nature. 2014;513(7517):202-9. doi: 10.1038/nature13480.
65. Wu X, Li X, Fu Q, Cao Q, Chen X, Wang M, et al. AKR1B1 promotes basal-like breast cancer progression by a positive feedback loop that activates the EMT program. The Journal of Experimental Medicine. 2017;214(4):1065-79. doi: 10.1084/jem.20160903.
66. Varadhachary GR, Abbruzzese JL, Lenzi R. Diagnostic strategies for unknown primary cancer. Cancer. 2004;100(9):1776-85. Epub 2004/04/28. doi: 10.1002/cncr.20202. PubMed PMID: 15112256.
67. Fizazi K, Greco FA, Pavlidis N, Daugaard G, Oien K, Pentheroudakis G, et al. Cancers of unknown primary site: ESMO Clinical Practice Guidelines for diagnosis, treatment and follow-up. Ann Oncol. 2015;26 Suppl 5:v133-8. Epub 2015/09/01. doi: 10.1093/annonc/mdv305. PubMed PMID: 26314775.
68. Lee J, Hahn S, Kim DW, Kim J, Kang SN, Rha SY, et al. Evaluation of survival benefits by platinums and taxanes for an unfavourable subset of carcinoma of unknown primary: a systematic review and meta-analysis. Br J Cancer. 2013;108(1):39-48. Epub 2012/11/24. doi: 10.1038/bjc.2012.516. PubMed PMID: 23175147; PubMed Central PMCID: PMC3553519.
69. Chen Y, Sun J, Huang L-C, Xu H, Zhao Z. Classification of Cancer Primary Sites Using Machine Learning and Somatic Mutations. BioMed Research International. 2015;2015:1-9. doi: 10.1155/2015/491502.
70. Leong HS, Galletta L, Etemadmoghadam D, George J, Australian Ovarian Cancer S, Kobel M, et al. Efficient molecular subtype classification of high-grade serous ovarian cancer. J Pathol. 2015;236(3):272-7. Epub 2015/03/27. doi: 10.1002/path.4536. PubMed PMID: 25810134.

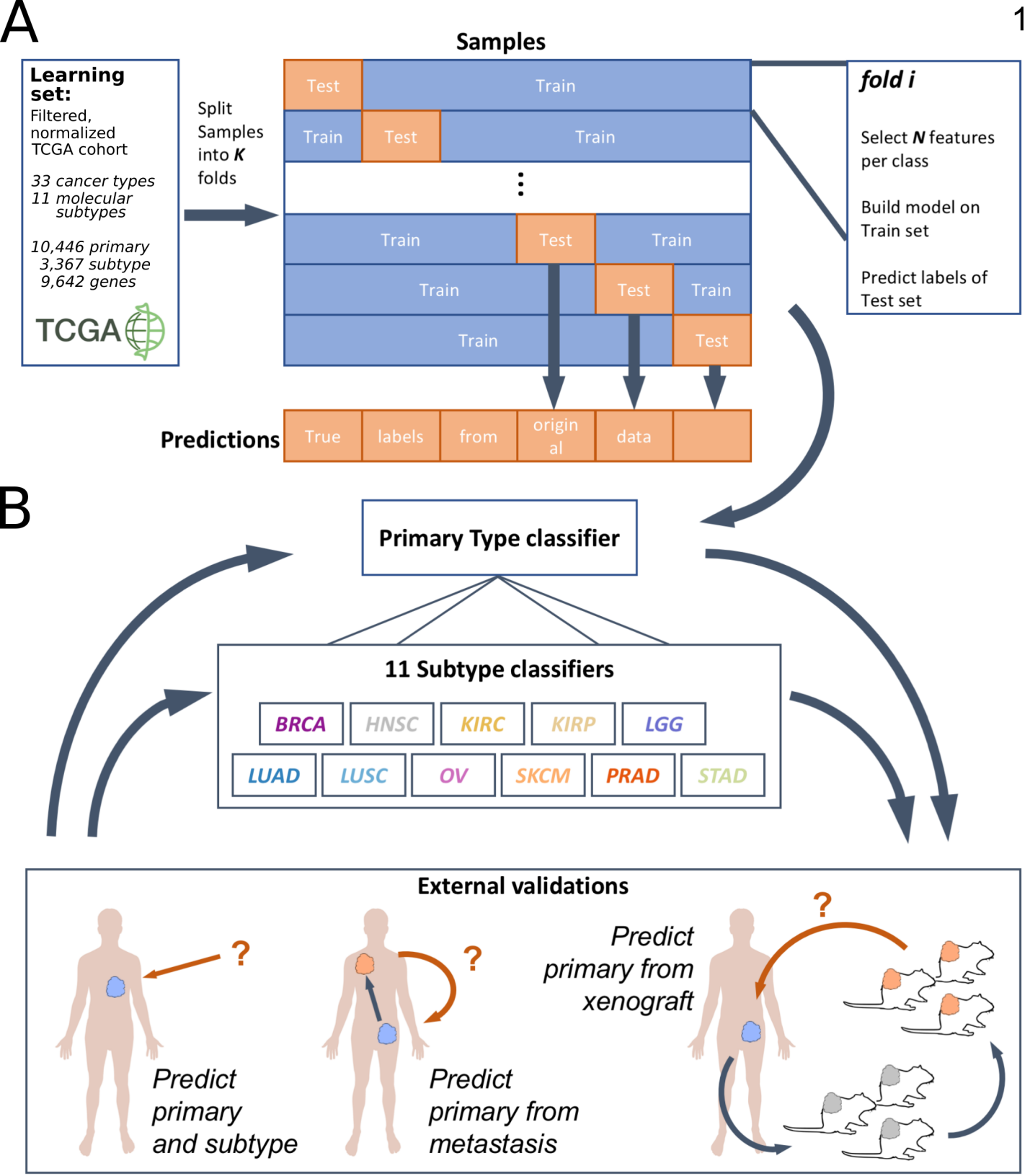
A
Samples
Learning set:
Filtered, normalized TCGA cohort
33 cancer types
11 molecular subtypes
10,446 primary
3,367 subtype
9,642 genes
TCGA
Split Samples into K folds
Test
Train
fold i
Select N features per class
Build model on Train set
Predict labels of Test set
Predictions
True labels from original data
B
Primary Type classifier
11 Subtype classifiers
BRCA
HNSC
KIRC
KIRP
LGG
LUAD
LUSC
OV
SKCM
PRAD
STAD
External validations
Predict primary and subtype
Predict primary from metastasis
Predict primary from xenograft

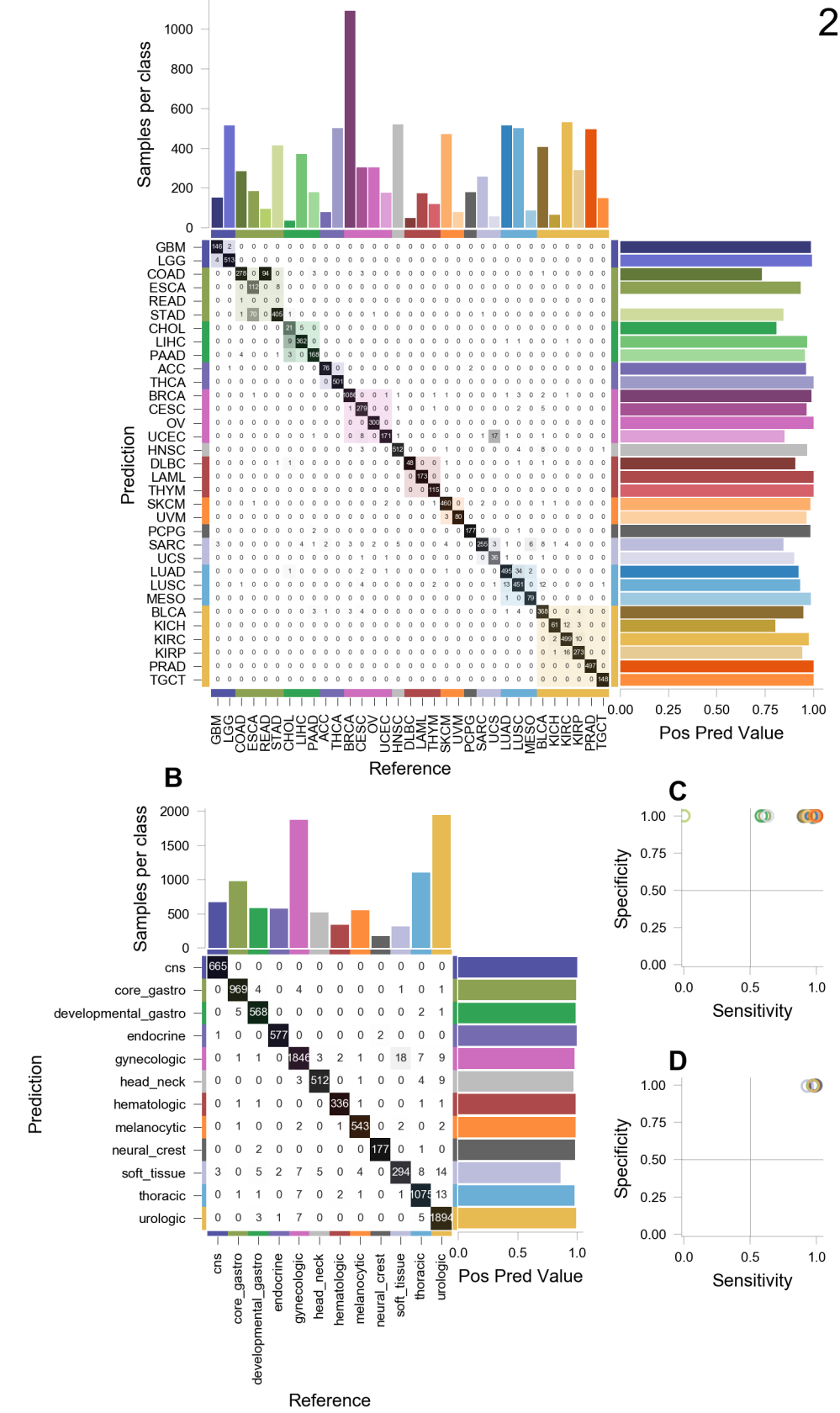
2
Samples per class
Prediction
Reference
Pos Pred Value
GBM
LGG
COAD
ESCA
READ
STAD
CHOL
LIHC
PAAD
ACC
THCA
BRCA
CESC
OV
UCEC
HNSC
DLBC
LAML
THYM
SKCM
UVM
PCPG
SARC
UCS
LUAD
LUSC
MESO
BLCA
KICH
KIRC
KIRP
PRAD
TGCT
B
Samples per class
Prediction
Reference
Pos Pred Value
cns
core_gastro
developmental_gastro
endocrine
gynecologic
head_neck
hematologic
melanocytic
neural_crest
soft_tissue
thoracic
urologic
C
Specificity
Sensitivity
D
Specificity
Sensitivity

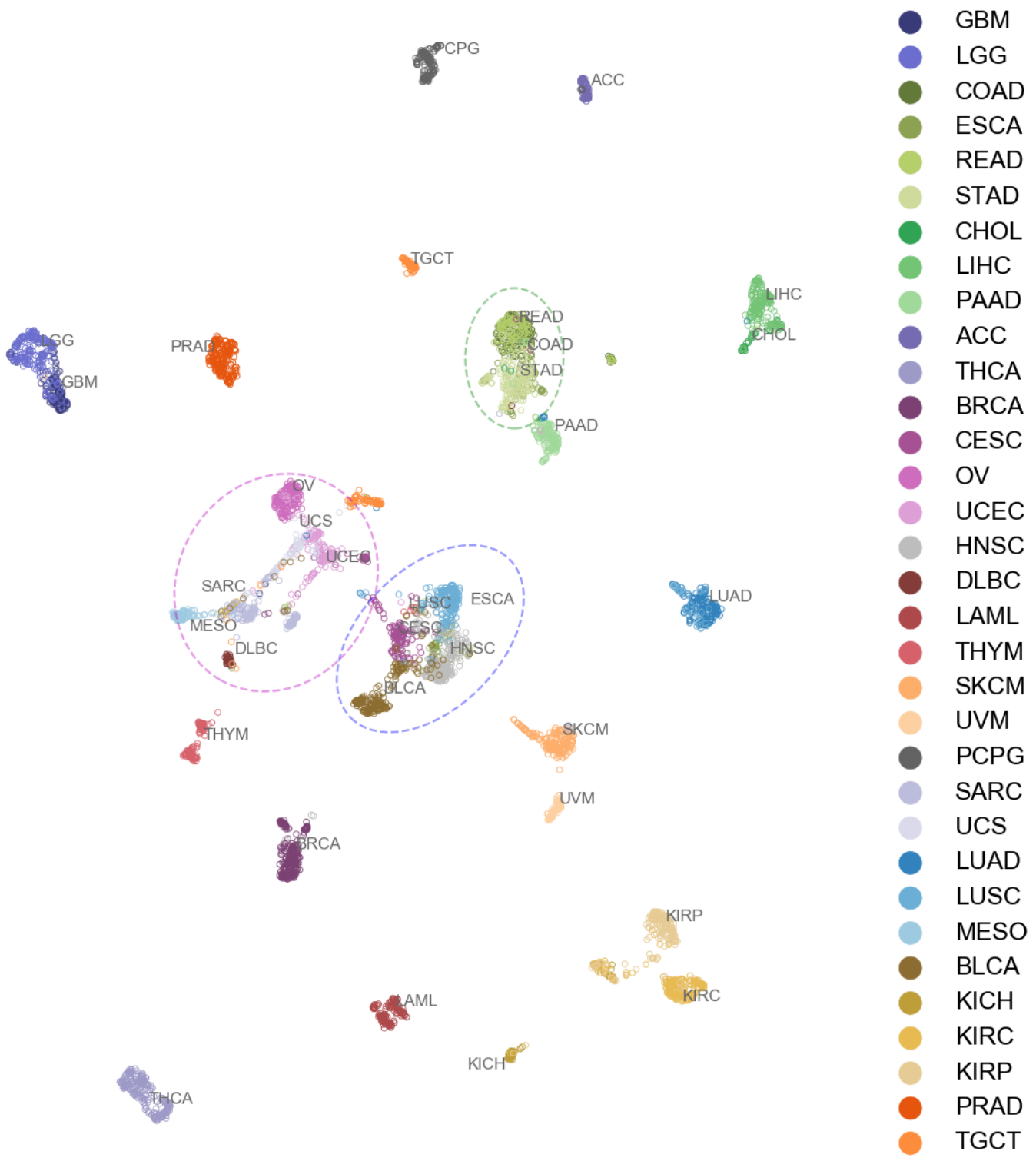
PCPG
ACC
TGCT
LIHC
CHOL
READ
COAD
STAD
PAAD
LGG
GBM
PRAD
OV
UCS
UCEC
SARC
MESO
DLBC
LUSC
ESCA
CESC
HNSC
BLCA
LUAD
THYM
SKCM
UVM
BRCA
KIRP
KIRC
LAML
KICH
THCA
GBM
LGG
COAD
ESCA
READ
STAD
CHOL
LIHC
PAAD
ACC
THCA
BRCA
CESC
OV
UCEC
HNSC
DLBC
LAML
THYM
SKCM
UVM
PCPG
SARC
UCS
LUAD
LUSC
MESO
BLCA
KICH
KIRC
KIRP
PRAD
TGCT

3

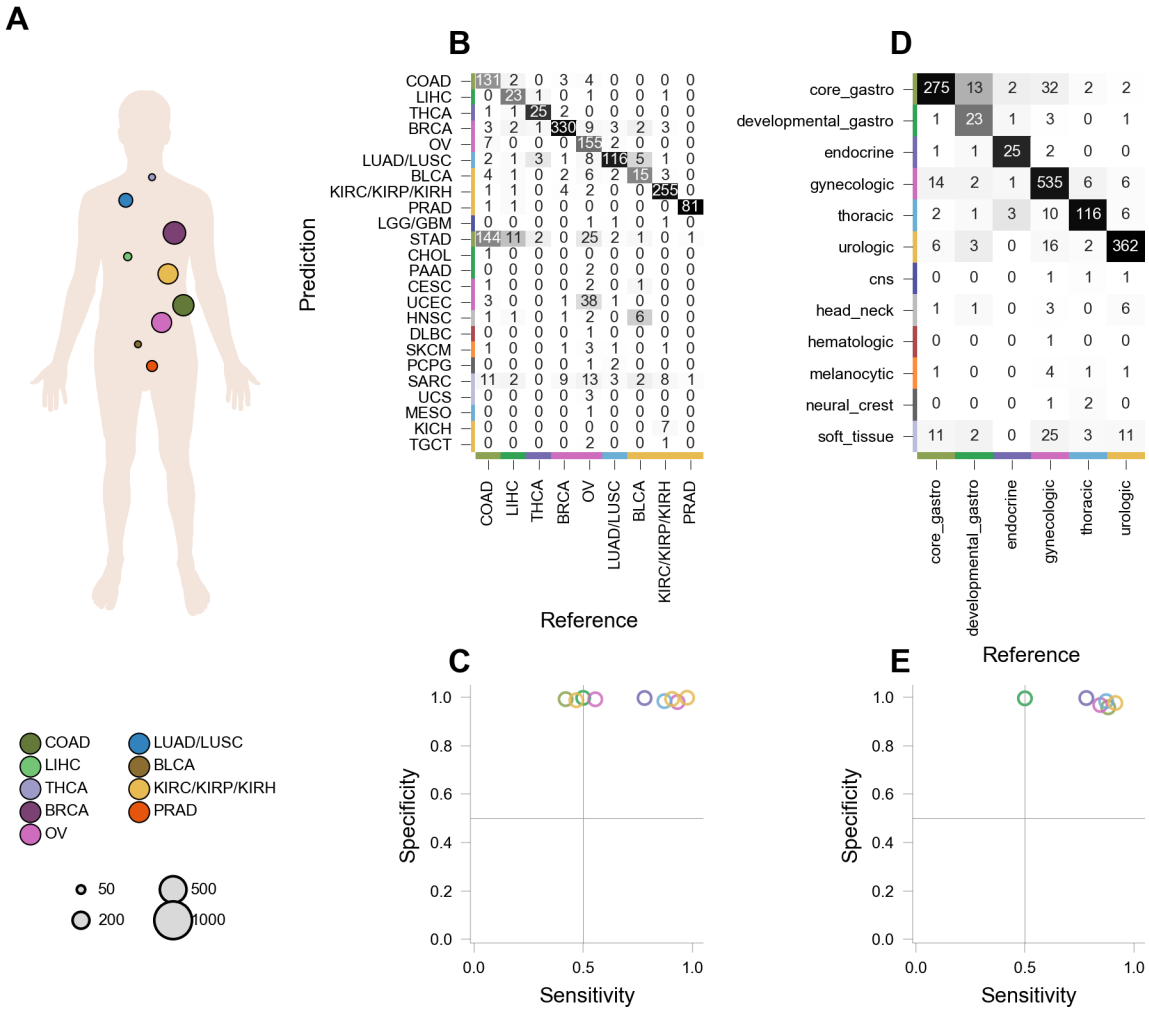
A
B
Prediction
Reference
COAD
LIHC
THCA
BRCA
OV
LUAD/LUSC
BLCA
KIRC/KIRP/KIRH
PRAD
LGG/GBM
STAD
CHOL
PAAD
CESC
UCEC
HNSC
DLBC
SKCM
PCPG
SARC
UCS
MESO
KICH
TGCT
D
core_gastro
developmental_gastro
endocrine
gynecologic
thoracic
urologic
cns
head_neck
hematologic
melanocytic
neural_crest
soft_tissue
C
E
Specificity
Sensitivity
LUAD/LUSC
BLCA
KIRC/KIRP/KIRH
PRAD
50
200
500
1000

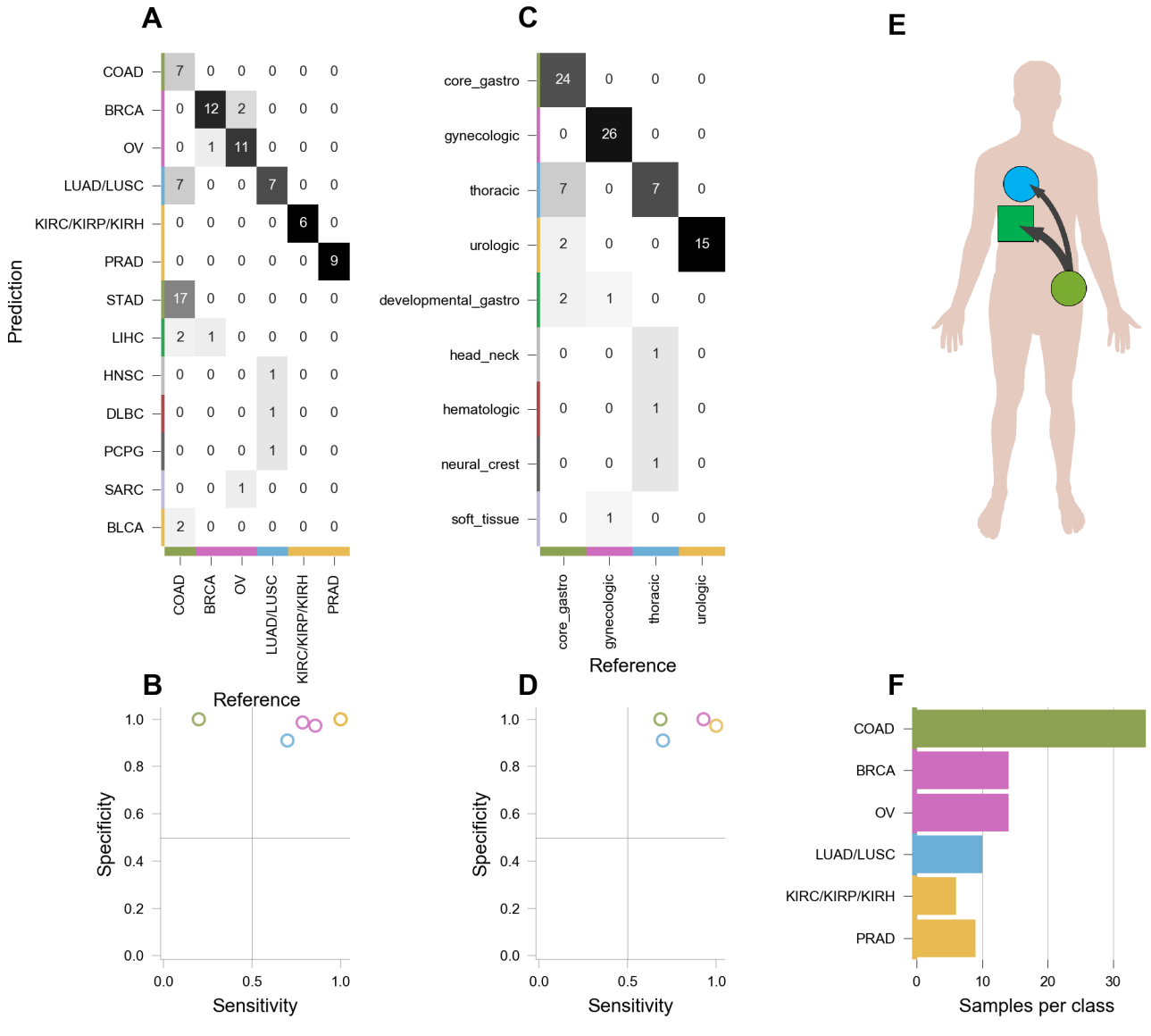
A
Prediction
COAD 7 0 0 0 0 0
BRCA 0 12 2 0 0 0
OV 0 1 11 0 0 0
LUAD/LUSC 7 0 0 7 0 0
KIRC/KIRP/KIRH 0 0 0 0 6 0
PRAD 0 0 0 0 0 9
STAD 17 0 0 0 0 0
LIHC 2 1 0 0 0 0
HNSC 0 0 0 1 0 0
DLBC 0 0 0 1 0 0
PCPG 0 0 0 1 0 0
SARC 0 0 1 0 0 0
BLCA 2 0 0 0 0 0
COAD BRCA OV LUAD/LUSC KIRC/KIRP/KIRH PRAD
C
core_gastro 24 0 0 0
gynecologic 0 26 0 0
thoracic 7 0 7 0
urologic 2 0 0 15
developmental_gastro 2 1 0 0
head_neck 0 0 1 0
hematologic 0 0 1 0
neural_crest 0 0 1 0
soft_tissue 0 1 0 0
core_gastro gynecologic thoracic urologic
Reference
E
B
Reference
Specificity
Sensitivity
0.0 0.2 0.4 0.6 0.8 1.0
D
Specificity
Sensitivity
0.0 0.2 0.4 0.6 0.8 1.0
F
COAD
BRCA
OV
LUAD/LUSC
KIRC/KIRP/KIRH
PRAD
0 10 20 30
Samples per class

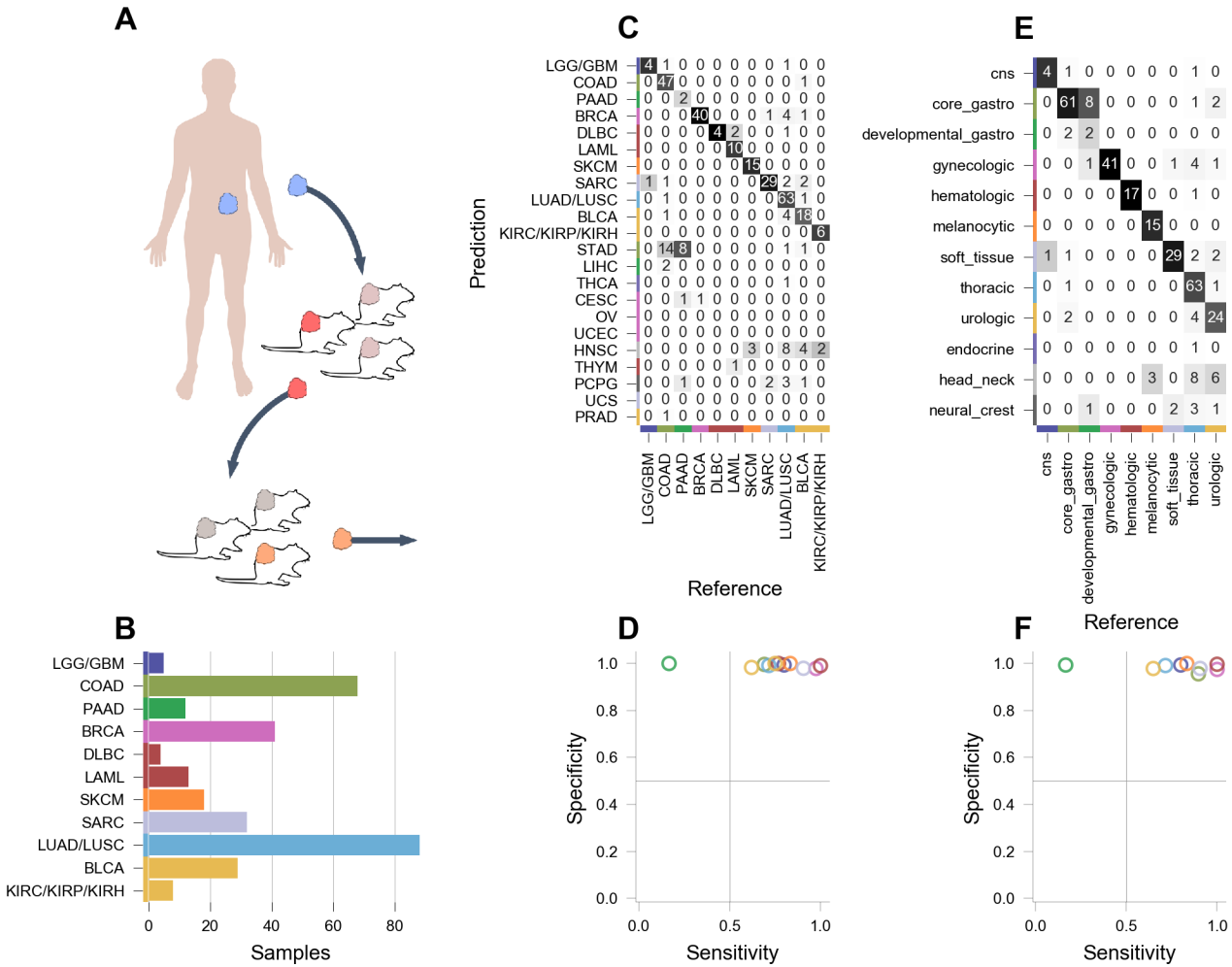
A
B
C
D
E
F
LGG/GBM
COAD
PAAD
BRCA
DLBC
LAML
SKCM
SARC
LUAD/LUSC
BLCA
KIRC/KIRP/KIRH
Samples
Prediction
Reference
Specificity
Sensitivity
cns
core_gastro
developmental_gastro
gynecologic
hematologic
melanocytic
soft_tissue
thoracic
urologic
endocrine
head_neck
neural_crest

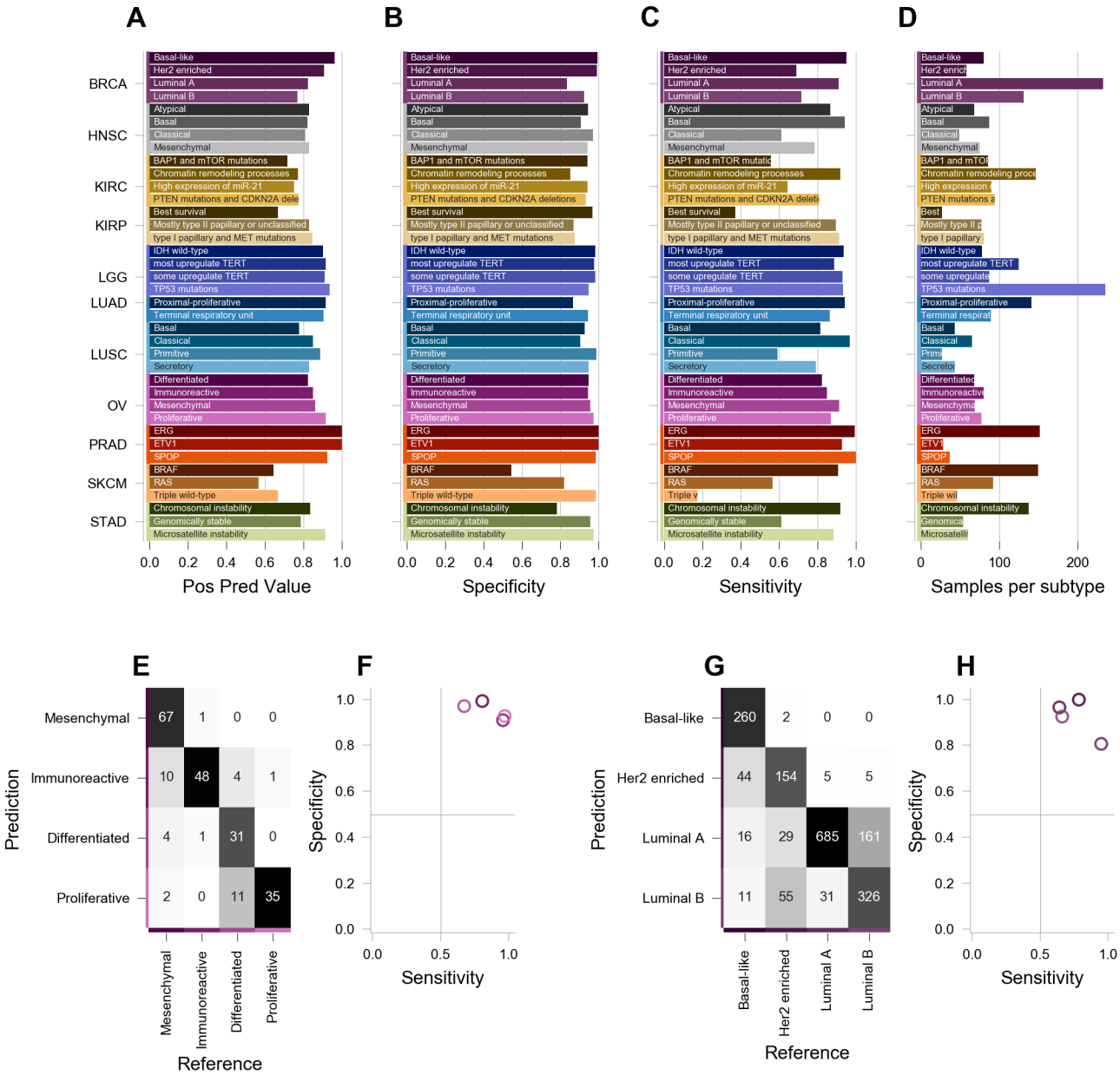
A
B
C
D
BRCA
HNSC
KIRC
KIRP
LGG
LUAD
LUSC
OV
PRAD
SKCM
STAD
Basal-like
Her2 enriched
Luminal A
Luminal B
Atypical
Basal
Classical
Mesenchymal
BAP1 and mTOR mutations
Chromatin remodeling processes
High expression of miR-21
PTEN mutations and CDKN2A deletions
Best survival
Mostly type II papillary or unclassified
type I papillary and MET mutations
IDH wild-type
most upregulate TERT
some upregulate TERT
TP53 mutations
Proximal-proliferative
Terminal respiratory unit
Primitive
Secretory
Differentiated
Immunoreactive
Proliferative
ERG
ETV1
SPOP
BRAF
RAS
Triple wild-type
Chromosomal instability
Genomically stable
Microsatellite instability
0.0 0.2 0.4 0.6 0.8 1.0
Pos Pred Value
Specificity
Sensitivity
0 100 200
Samples per subtype
E
Prediction
Mesenchymal 67 1 0 0
Immunoreactive 10 48 4 1
Differentiated 4 1 31 0
Proliferative 2 0 11 35
Mesenchymal
Immunoreactive
Differentiated
Proliferative
Reference
F
Specificity
Sensitivity
G
Prediction
Basal-like 260 2 0 0
Her2 enriched 44 154 5 5
Luminal A 16 29 685 161
Luminal B 11 55 31 326
Basal-like
Her2 enriched
Luminal A
Luminal B
Reference
H
Specificity
Sensitivity